AN ITERATIVE METHOD IN DYNAMIC STRUCTURAL ANALYSES WITH NONPROPORTIONAL DAMPING

Wan T. Tsai[1], Joseph T. Leang[2]

ABSTRACT

A new method in dynamic analyses of structures with non-proportional damping is proposed. By decomposing the non-proportional damping matrix into two portions, the diagonal and off-diagonal, the iterative technique can be employed through use of the classic method of solving a large dynamic structural system with real modal coordinates. Explicitly, the diagonalized damping matrix is retained to form a system of discrete differential equations with proportional damping. The off-diagonal portion of damping forces is treated as a correcting forcing function. The iteration is to use the off-diagonal damping induced forces for the load correction in the subsequent computational step. This enables the structural responses to be simply determined while the effect of off-diagonal damping forces is included.

---

[1]MTS, Dynamic Loads, Rockwell Int'l, 12214 Lakewood Blvd., Mail Code AD88, Downey, CA 90241, (213) 922-0570. Also, Adjunct Professor, Mechanical Engineering Dept., Calif. State Univ., Long Beach.

[2]MTS, Dynamic Loads, Rockwell Int'l, 12214 Lakewood Blvd., Mail Code AD88, Downey, CA 90241, (213) 922-5794.

AN ITERATIVE METHOD IN DYNAMIC STRUCTURAL ANALYSES WITH NONPROPRTIONAL DAMPING

Wan T. Tsai, J. T. Leang
Dynamic Loads, Rockwell International, Downey, CA

INTRODUCTION

This article presents a new method in dynamic analyses of structures with non-proportional damping. Computed iteratively, this method ensures highly accurate responses yet low cost analyses when the structures are subjected to dynamic forcing functions.

In dynamic analyses of space vehicles, the mass and stiffness matrices of each substructure are usually generated by different contractors. Each substructure may contain its own component modal damping acquired from component testing or empirical data. When all substructures are coupled together into a system for dynamic analyses, a difficulty arises. Generally, the system damping matrix cannot be transformed into a diagonal matrix by using the same transformation matrix as for generalizations of the system mass and stiffness matrices. Since the transformed damping matrix is not diagonalized, the structural responses cannot be determined by taking the advantage of using the real mode superposition technique. In order to avoid this difficulty, the off-diagonal elements of the transformed damping matrix are usually neglected in the wake of their smallness compared to the corresponding diagonal elements. Known as triple-matrix-product (TMP) method in the aerospace industry, this approach has been widely employed as a standard method in analyses of space vehicles. Using this approach, the interface loads are usually accurate for design purposes. However, the responses in some payload components may be grossly incorrect when the full scale payload-orbiter coupled systems are exercised.

The proposed iterative method is to improve the accuracy of payload responses yet to retain the advantage of using the modal superposition technique for cost saving. This method decomposes the transformed system modal damping matrix into two portions, a diagonal damping matrix and an off-diagonal damping matrix. The damping force induced by the off-diagonal damping elements are treated as a correcting force vector to modify the applied forcing function. This correction can be repeatedly applied until the results are within an acceptible range of error. Using this iterative approach, the desired goal can be reached and the impact to the currently applied TMP method can be minimized.

The iterative method in treating the nonproportional damping matrix has been applied by the first author of this paper to analyze small scale of structures since 1988. Independently, the same method given by Udwadia and Esfandiari (1990), may be the first article related to this method published in the open literature. The convergent characteristics of the method is the primary emphasis of the article. Prior to using the iterative method, several approaches have been proposed in treating structural systems with non-proportional damping. Primarily due to the development of nuclear power plants in the 1970s, replacements of the non-proportional damping matrix with diagonal matrix have been extensively investigated. Those which have been more commonly employed are: (1) using the diagonal elements of the non-proportional damping matrix, i.e., the triple-matrix-product (TMP) method, (2) replacing the non-proportional damping matrix by a diagonal matrix containing each element with a factor of the critical damping to each mode, i.e., the system damping method, and (3) obtaining each diagonal damping element by using the algebraic sum of the corresponding row of the non-proportional damping matrix. Errors acquired from these approximations had also been examined. Those who had been involved in these methodology developments included Clough and Mojtahedi (1976), Cronin (1976), Duncan and Taylor (1979), Hasselman (1976), Thompson, Calkin, and Caravani (1974), and Warburton and Soni (1977.) A different approach in synthesizing the diagonal system damping elements from the component modal testing was given by Tsai (1989.) It is known that a non-proportionally damped system can be completely generalized through the complex mode transformations. Many investigators have been involved in developments of this method, for instance, Beliveau and Soucy (1985), and Veletsos and Ventura (1986.) Although, the complex mode transformation is the exact method in treating non-proportionally damped structural systems, the real mode transformation seems to be still more favorable to most application engineers for two reasons: (1) It is less costly in the full scale transient analysis when an approximate method is employed. (2) It is easier to capture the image of physical behavior when the real mode transformation is applied. Therefore, the approximations developed in the 1970s are still favorably used. The TMP and the system damping approaches have been particularly favored in the aerospace industry.

In addition to the derivation of the iterative method, this paper emphasizes on case applications of the method to a full scale payload/orbiter dynamic analysis, i.e., the IUS/TDRS payload for the 26th space transportation system (STS-26) manifest. The direct integration method is employed as the basis to substantiate the validity of the new method. The reason that the TMP method is inadequate for payload response computations is extensively discussed. Recommendations in transient analyses for non-proportionally damped structures are provided.

ITERATIVE METHOD

Let M, C, and K be the physically coupled mass, damping, and stiffness matrices, P the applied forcing vector, X the response vector, and dots the derivatives with respect to time; the governing differential equation of the dynamic system is given by

$$M\ddot{X} + C\dot{X} + KX = P \tag{1}$$

Eq.(1) can be solved in a simple manner by transforming the physical response coordinates X into a system of generalized response coordinates x by introducing a transformation matrix φ. Namely

$$X = \varphi x \tag{2}$$

Through use of Eq.(2), along with the correlations

$$m = \varphi^T M\varphi, \quad c = \varphi^T C\varphi, \quad k = \varphi^T K\varphi, \quad p = \varphi^T P \tag{3a,b,c,d}$$

Eq.(1) then reduces to

$$m\ddot{x} + c\dot{x} + kx = p \tag{1'}$$

where, m is a unit matrix, c is a fully populated matrix, k is a diagonal matrix containing eigenvalues in the diagonal elements, and p is a generalized forcing vector.

Eq.(1') could be easily solved by using the real mode superpositions if c were a diagonal matrix. In order to take the advantage of expressing all responses with the superpositions of real modes, let c be expressed by the sum of a diagonal matrix c_d and an off-diagonal matrix c_o. Namely,

$$c = c_d + c_o \tag{4}$$

Eq.(1') can then be rewritten by

$$m\ddot{x} + c_d\dot{x} + kx = p - c_o\dot{x} \tag{5}$$

Thus, all the coefficient matrices on the left hand side of Eq.(5) are diagonal. The contribution of each generalized mode can be directly determined without coupling with the other modes. The technique of modal superpositions can then be applied to simplify the analysis inasmuch as the forcing function vector on the right hand side is explicitly given. The industrial practices generally assume that the effect of c_o is negligible since its elements are generally smaller than the corresponding elements of c_d. The approach using this assumption is the method commonly referred in the aerospace industry as the triple-matrix-product (TMP). In fact, the words triple-matrix-product (TMP) does not comprise any meaning of stripping the off-diagonal damping elements. Nevertheless, this article uses the commonly accepted definition that the TMP method implies the applications of the diagonalized damping matrix.

Now, the iterative method comes to play by treating the response vector x on both sides of Eq.(5) as if they were independent at different stages of computations, x_n and x_{n-1}, where n is the number of iterations. Eq.(5) is then rewritten into the form

$$\ddot{x}_n + c_d \dot{x}_n + k x_n = p - c_o \dot{x}_{n-1}, \quad n = 0,1,2,\ldots \tag{6}$$

The left hand side represents the classic modal system of equations whereas the right hand side is the forcing function corrected by the off-diagonal damping induced forces. Using this system of equations, the modal DOFs can be easily determined since every equation is associated with a single DOF.

In Eq.(6), $\dot{x}_{-1}=0$ when n=0. The response x_0 is the TMP result. The off-diagonal damping force obtained from the TMP result is applied to modify the applied force and the first iterative response x_1 for n=1 is then determined from Eq.(6). Analogously, the second iterative response x_2 for n=2 is computed by using the correcting force obtained from the x_1 response. This procedure can be repeatedly applied until the nth iterative response x_n reaches an acceptible accuracy.

The iteration can be stopped when the response converges to a desired accuracy. Using various examples of three degree-of-freedom, Udwadia and Esfandiari showed that the results of six iterations were almost identical to the exact solutions. For practical applications, such a highly accurate result may not be necessary. The analysis may be terminated by setting an accuracy criterion that the converging rate of the modal accelerations is within a specified admissible error, ε. Namely,

$$\left| \frac{\ddot{x}_{n-1}}{\ddot{x}_n} - 1 \right| < \varepsilon, \quad n = 1,2,\ldots \tag{7}$$

For most design purposes, the modal accelerations may be accurate enough to assume an admissible error of 5% (0.05). This value is suggested on the basis of common practices, not a sophisticatedly computed number. Experiences indicate that responses may generally be converged to $\varepsilon<0.05$ when two iterations are performed.

It must be noted that the provided error limit for the modal accelerations does not assure of the physical accelerations to be always within the same limit. However, their limits are generally agreeable to each other in most applications. It must also be noted that the error determined by Eq.(7) is to judge the acceleration computed in the (n-1)th iterative analysis with the nth iterative acceleration as the basis. In fact, when the result of the nth iteration is used for final response evaluation, the accuracy is higher than the specified admissible error since the updated result is supposed to be judged with the (n+1)th iterative values.

APPLICATIONS OF ITERATIVE METHOD

The dynamic liftoff analysis for the STS-26 flight manifest was used to demonstrate applications of the iterative method. The manifest consists of the substructures: tracking data relay satellite (TDRS), inner upper stage (IUS) booster, orbiter, solid rocket booster (SRB), and external tank (ET). The spacecraft TDRS was integrated to the IUS which was in turn secured to the orbter cargo bay through payload trunnions. The primary purpose of this flight was to deploy the payload IUS/TDRS.

Originally, all components were individually modelled as substructures, each was represented by hundreds or thousands of degree-of-freedoms (DOFs). After several stages of substructural coupling and condensations, the final model used for the liftoff dynamic analyses was 520 DOFs. The system was subjected to a dynamic forcing function, LR1200, one of the conditions being used for liftoff transient analyses. The analysis was performed over a range of 11 seconds to cover the complete liftoff event. To assure of obtaining an accurate result, the small time interval of 0.001 seconds was used over the entire time span of transient analyses. In the dynamic loads analysis, 1% of the critical damping was assumed for all the IUS/TDRS payload modes. For the orbiter, 1% for frequencies below 10Hz and 2% for frequencies above 10Hz were assumed. No damping was assumed at the payload/orbiter interface DOFs. The analyses were performed by using various approaches for comparisons. The results are summarized in Tables 1-5 in which column 1 represents the items of interest. Columns 2-6 represent the minimum and maximum values obtained from various methods of transient analyses.

Initially, the dynamic system was analyzed by using the TMP method. The results are summarized in column 2 of Tables 1-5 for various component responses. The accelerations along the X-direction at the tip of SA antenna ribs (node 115) was excessively high, a minimum of -25.7g and a maximum of 27.2g as shown in column 2 of Table 1. Since this result was not acceptible and such a strong response was very unusual, a similar analysis was performed by using 1% of the critical system damping. As shown in column 6 of Table 1, the response for the same item reduces significantly to a minimum of -9.6g and a maximum of 9.2g. Clearly, the comparison between these two sets of results indicates a controversial conclusion that the system with a higher damping value has a stronger response than the one with a lower damping value. This conclusion violates the nature of mechanics that a structure has less responses with higher damping.

When the iterative method is applied, the peak accelerations of the same item become -6.8g and 7.4g for one iteration, and -7.2g and 7.7g for two iterations. These results are respectively shown in columns 3 and 4 of Table 1. They are significantly different from that of the TMP method. The responses of several other items are also significantly changed between the TMP and iterative methods. For instance, the Y-acceleration of the C-band reflector CG in Table 1 and the member force at the LTM row 149 in Table 2, their responses using the iterative method appear to be less than one-half the TMP results. The difference between these selected items reveal a fundamentally severe deviation between the TMP and iterative methods, although the responses of many other items are in good agreement. Physically, the results obtained from the iterative method make better sense than from the TMP method when they are compared to those using the system damping method, as shown in column 6 of Tables 1-5.

To make sure that the iteratively computed results are reasonably accurate, the first iterative result is compared to the second one, i.e., column 3 compared to column 4 of Tables 1-5. Among all interested items, the maximum difference between these two iterative analyses is only 4.6% occured in the X-acceleration at the tip of SA antenna ribs. Furthermore, in order to assure of correct results obtained from the iterative analyses, a direct integration method using the fully populated damping matrix is also performed. The results are shown in column 5 of Tables 1-5. All iterative responses are in very good agreement with the direct integration results. In general, the results of the second iteration are much closer to that of the direct integration than those of the first iteration. In certain particular items such as the tip of SA antenna ribs, the second iterative value has slightly more deviation than the first iterative result when both are compared to the direct integration result. It just happens on the way of converging process to the final result, but does not indicate any inaccuracy in the iterative method.

A question has been raised regarding the magnitude of the interface loads between using the system damping and iterative methods. Specifically, the load of -8909 lbs in the 1% system damping analysis appear to be weaker than -9024 lbs of the iterative analysis for the X-interface load at X=1155.53 inches (node 43.) This may not be surprised since the damping matrix established for the iterative method is more complex than that for the system damping matix. The one for the iterative analysis consists of zero damping value at the inteface nodes as well as 1% and 2% for the Craig-Bamptom form of substructure modelling. But the 1% system damping implicitly include damping values at the interface nodes as well as the other DOFs, as shown in the reversed expression of Eq.(3b). This explains the reason that some of the interface loads are stronger in the iterative analyses than in the analysis of using 1% system damping. The discrepancy for most of other quantities appears to be in the right order that the responses using the system damping method (1% damping) is slightly greater than those using the iterative method (1% and 2% damping for orbiter.)

REASONS FOR THE RESPONSE DISCREPANCY OF TMP METHOD

The reason for such a significant deviation in the TMP method has been interpreted as the consequence of modal response superpositions from two modes that have two closely spaced modes. This can be explained by considering the modal contribution for an item at a particular time slice. For instance, the modal contributions of the acceleration at the tip of SA antenna ribs at t=8.3 second are shown in Figures 1 and 2 respectively for the TMP and one-iterative analyses. Although both modal contribution plots appear to be different, the major contributions occur at the same frequency of 25.4Hz in either analyses. Near the interested frequency, the contributions from Figure 1 of the TMP approach are both negative whereas the contributions from Figure 2 of the iterative method are mixed with a negative and a positive value. Owing to this type of misrepresentation in the TMP modal contributions, the TMP computed responses become significantly different from those of the iterative analysis.

Although the above interpretation is mathematically correct, there remains a clout regarding the true driving source that causes such a strong impact to the component responses in the present illustration. A careful study indicates that the light weight flexible components are driven by wrong forces when the TMP approach is applied. That is the true reason to induce such a significant impact at the component responses. This can be directly interpreted by using Eq.(5). Since the generalized mass m is a unit matrix, Eq.(5) can be rewritten into an alternate form to express the acceleration in terms of p, k, c_o, c_d, x, and $\dot{x}$. The acceleration for the ith modal DOF is given by

$$\ddot{x}_i = p_i - k_i x_i - (c_d)_i \dot{x}_i - \sum_j (c_o)_{ij} \dot{x}_j \tag{8}$$

In the TMP analysis, the last term associated with c_o has been entirely neglected. This may be justified when the applied force p_i, stiffness force $k_i x_i$, and diagonal damping force $(c_d)_i \dot{x}_i$ are much greater than the total off-diagonal damping force. For the internal components of a payload, the DOFs are generally not subjected to any directly applied forces. Instead, the component DOFs are driven by the combined action of stiffness and damping forces. When the stiffness is relatively small like the SA antenna ribs[1], the associated stiffness force is small and the damping force becomes an important part of the driving force. Furthermore, the off-diagonal damping force becomes the dominated portion in the total driving force. Specifically, the sum of several hundreds of off-diagonal damping force components may override the stiffness and diagonal damping forces to influence the final responses of the transient analysis, although each off-diagonal damping force component may be small compared to the counterpart of the stiffness and diagonal damping forces.

---

[1]The component stiffness is small compared to the other portion of the structural system. However, the component frequency may not be small since the corresponding component mass is usually small too.

The above interpretation can be substantiated by the TDRS member loads shown in Table 2. The item at the LTM row 149 has a peak member force reduced from 21.7 lbs in the TMP approach down to 11.9 lbs in the one-iterative analysis. Similarly, the small IUS motor (node 3457) has the peak Y-acceleration changed from 0.42g to 0.23g as shown in Table 4. The changes are up to 100%. On the contrary, the changes in the interface loads at the bridge points between the IUS/TDRS and orbiter as shown in Table 3 and the orbiter bridge acceleration as shown in Table 5 are much less, a maximum of 13% only. Therefore, the TMP may still be applicable if all substructural components are stiff. However, when the component is flexible, it may be subjected to a wrong driving force when the off-diagonal damping force is neglected. As a result, the component response is incorrect. It is particularly sensitive to the component of small mass since it is more responsive to any variation of the driving force.

CONCLUSIONS

1. The commonly referred TMP method has assumed that the off-diagonal damping elements are small and negligible; and that uses of the diagonal damping elements are sufficient to capture accurate component responses of structures. This has been proved to be incorrect. In fact, the TMP method may produce a structural response totally different from the true result. Therefore, the currently applied TMP method should not be used.

2. A new method using iterative procedure is proposed for transient analyses of dynamic structures with non-proportional damping. This method can provide an accurate result within small number of iterations. The validity of this method has been substantiated by using the direct integration method through the illustrative analyses for the STS-26 flight.

3. The proposed iterative method is cost effective. On the basis of analyses for various structure sizes, the cost of using each additional iteration is about 15% more than the cost of using the TMP approach. Generally, two iterations may result in an accurate response for design purposes. If two iterations are used, the expected computing cost may increase about 30%. This cost is not a significant impact when it can assure of obtaining a reliable response in all payload components. Therefore, the iterative method is a viable approach for transient analyses when the transformed system damping matrix is non-proportional.

RECOMMENDATIONS

To ensure accurate component responses of structures, the off-diagonal damping elements must <u>not</u> be neglected. In order to retain the off-diagonal damping without significantly increasing computational cost, the iterative method may be used.

ACKNOWLEDGMENT

The authors wish to thank Dr. R. S. Chao for his encouragement in preparation of this article. They are also grateful for the reference search and technical discussions of Dr. H. T. Tang of Electric Power Research Institute and Dr. C. S. Lin of the Aerospace Corporation.

REFERENCES

Beliveau, J. G., Soucy, Y., 1985, "Damping Synthesis Using Complex Substructure Modes and A Hermitian System Representation," AIAA 26th Structures, Structural Dynamics, and Material Conference, paper No. 85-0785, pp. 581-586.

Clough, R. W., Mojtahedi, S., 1976, "Earthquake Response Analysis Considering Non-Proportional Damping," Earthquake Engineering and Structural Dynamics, Vol. 4, pp. 489-496.

Cronin, D. L., 1976, "Approximation for Determining Harmonically Excited Response of Non-Classically Damped Systems," ASME J. Engineering for Industry, pp. 43-47.

Duncan, P. E., Taylor, R. E., 1979, "A Note on The Dynamic Analysis of Non-Proportionally Damped Systems," Earthquake Engineering and Structural Dynamics, Vol. 7, pp. 99-105.

Hasselman, T. K., 1976, "Modal Coupling in Lightly Damped Structures," AIAA J., Vol. 14, pp. 1627-1628.

Thompson, W. T., Calkins, T., Caravan, P., 1974, "A Numerical Study of Damping," Earthquake Engineering and Structural Dynamics, Vol. 3, pp. 97-103.

Tsai, W., 1989, "Considerations of Synthesized System Damping in Dynamic Analysis of Space Structures," Proceedings of Damping'89, 8-10, February 1989, West Palm Beach, Fl., pp. DBE.1-DBE.13.

Udwadia, F. E., Esfandiari, R. S., 1990, "Nonclassically Damped Dynamic System: An Iterative Approach," J. Appl. Mech., Vol. 57, pp. 423-432.

Veletsos, A. S., Ventura, C. E., 1986, "Model Analysis of Non-Classically Damped Linear Systems," Earthquake Engineering and Structural Dynamics, Vol. 14, pp. 217-243.

Warburton, G. B., Soni, S. R., 1977, "Errors in Response Calculations for Non-Classically Damped Structures," Earthquake Engineering and Structural Dynamics, Vol. 5, pp. 365-376.

TABLE 1 STS-26 TDRS ACCELERATION (g)

1		2		3		4		5		6	
		Diagonal TMP		1 Iteration		2 Iterations		Full Damp-Matrix		1% System Damping	
ITEMS		Min	Max	Min	Max	Min	Max	Min	Max	Min	Max
SGL Antenna	# 13 X	-1.869	2.678	-1.842	2.812	-1.830	2.830	-1.836	2.831	-1.742	2.823
SGL Antenna	# 13 Y	-2.732	2.759	-2.755	2.818	-2.759	2.824	-2.761	2.825	-2.729	2.782
SGL Antenna	# 13 Z	0.300	3.355	0.220	3.288	0.216	3.290	0.216	3.289	0.189	3.352
SGL Feed	# 15 X	-2.868	3.590	-2.850	3.774	-2.842	3.782	-2.843	3.789	-2.798	3.652
SGL Feed	# 15 Y	-2.192	2.094	-2.226	2.128	-2.233	2.137	-2.236	2.139	-2.181	2.057
SGL Feed	# 15 Z	-2.380	4.475	-2.298	4.353	-2.306	4.350	-2.309	4.351	-2.317	4.394
C-Band Antenna	# 17 X	-4.607	4.534	-4.067	3.831	-3.973	3.785	-4.012	3.800	-3.952	3.905
C-Band Antenna	# 17 Y	-1.628	1.618	-1.208	1.240	-1.207	1.240	-1.207	1.239	-1.217	1.249
C-Band Antenna	# 17 Z	-2.883	5.601	-0.532	3.593	-0.524	3.602	-0.532	3.605	-0.564	4.039
C-Band Reflector CG	# 18 Y	-5.371	5.482	-2.297	2.268	-2.300	2.275	-2.301	2.282	-2.652	2.941
Top C-Band Antenna	# 20 X	-17.004	15.478	-14.429	13.682	-14.471	13.738	-14.391	13.689	-14.779	14.034
Top C-Band Antenna	# 20 Y	-7.164	7.223	-4.977	5.120	-5.002	5.144	-5.002	5.138	-5.034	5.261
Top C-Band Antenna	# 20 Z	-5.117	8.104	-1.120	4.128	-1.134	3.935	-1.135	3.786	-1.769	5.133
Propellant Tank CG	# 75 X	-0.814	1.028	-0.730	0.912	-0.728	0.911	-0.728	0.911	-0.721	0.917
Propellant Tank CG	# 75 Y	-0.510	0.453	-0.405	0.378	-0.416	0.379	-0.422	0.380	-0.505	0.477
Propellant Tank CG	# 75 Z	0.160	3.347	0.160	3.354	0.157	3.360	0.158	3.358	0.130	3.442
+Y Solar Panel Hinge	# 83 X	-4.582	3.507	-3.064	2.399	-3.001	2.377	-2.898	2.370	-3.557	3.091
+Y Solar Panel Hinge	# 83 Y	-2.762	2.802	-2.153	1.643	-2.157	1.643	-2.157	1.602	-2.285	1.981
+Y Solar Panel Boom	# 84 X	-1.114	1.191	-0.996	1.193	-0.993	1.202	-0.991	1.204	-1.118	1.269
+Y Solar Panel Boom	# 84 Y	-0.630	0.632	-0.514	0.540	-0.504	0.534	-0.503	0.537	-0.550	0.577
+X SA Antenna Ribs	#114 X	-15.354	16.508	-8.434	10.605	-8.486	10.687	-8.503	10.685	-8.686	11.969
+X SA Antenna Ribs	#114 Y	-10.779	11.661	-13.079	11.731	-13.151	11.865	-13.198	11.948	-20.363	20.347
+X SA Antenna Ribs	#115 X	-25.678	27.177	-6.820	7.402	-7.152	7.748	-7.010	7.303	-9.588	9.243
+X SA Antenna Ribs	#115 Y	-11.695	12.841	-12.517	14.087	-12.565	14.248	-12.590	14.302	-15.463	15.945

TABLE 2 STS-26 TDRS MEMBER FORCES (lbs)

1	2		3		4		5		6	
	Diagonal THP		1 Iteration		2 Iterations		Full Damp-Matrix		1% System Damping	
ITEMS	Min	Max	Min	Max	Min	Max	Min	Max	Min	Max
LTM Row 7	-31.352	167.415	0.742	157.726	0.716	158.092	0.617	158.080	-2.211	161.663
LTM Row 8	-96.063	97.823	-87.604	88.290	-87.553	88.306	-87.588	88.383	-86.971	86.844
LTM Row 9	-239.302	248.886	-244.731	251.355	-244.525	250.255	-244.563	250.720	-248.846	247.068
LTM Row 10	-3779.852	4048.862	-3714.292	3640.342	-3695.735	3621.714	-3698.991	3629.298	-3790.617	3638.845
LTM Row 11	-15316.294	15094.682	-15324.837	15111.364	-15323.642	15106.433	-15319.220	15105.144	-15111.047	14984.546
LTM Row 12	-6588.836	5736.225	-6561.235	5739.295	-6563.184	5741.535	-6563.380	5742.944	-6565.495	5721.129
LTM Row 13	-18.031	180.071	-16.874	172.224	-16.880	172.217	-17.039	172.166	-17.373	173.739
LTM Row 14	-138.362	133.735	-139.851	131.348	-140.204	131.659	-140.250	131.769	-138.204	132.125
LTM Row 15	-100.012	141.493	-99.980	150.813	-100.441	151.302	-100.627	151.444	-95.802	149.997
LTM Row 16	-2302.582	2691.156	-2302.934	2720.638	-2306.025	2709.896	-2306.691	2710.974	-2266.597	2597.696
LTM Row 17	-9965.971	6880.373	-10251.104	6822.615	-10267.150	6790.424	-10270.888	6801.434	-10180.191	6558.322
LTM Row 18	-12220.455	10234.987	-12191.952	10223.477	-12203.518	10212.594	-12209.673	10212.579	-12232.624	10284.899
LTM Row 49	-910.043	1097.881	-912.467	1100.754	-912.520	1101.126	-912.640	1101.521	-903.279	1093.266
LTM Row 50	-26.328	81.262	-24.331	80.765	-24.317	79.826	-24.691	79.748	-29.942	81.354
LTM Row 51	-80.621	92.894	-79.501	93.739	-79.559	93.806	-79.628	94.043	-81.248	94.451
LTM Row 52	-135.642	149.803	-136.405	144.737	-136.593	145.011	-137.038	145.010	-139.581	149.702
LTM Row 53	-201.294	397.658	-190.031	403.868	-190.372	404.094	-190.581	404.592	-194.017	397.817
LTM Row 54	-140.504	126.025	-132.522	120.977	-132.493	121.681	-131.217	121.498	-146.011	133.610
LTM Row 55	-123.781	77.939	-136.341	67.925	-137.451	68.019	-137.441	68.392	-147.906	71.118
LTM Row 56	-6.905	9.548	-6.711	9.667	-6.701	9.695	-6.668	9.694	-7.013	9.579
LTM Row 57	-959.580	1150.629	-967.793	1163.026	-967.470	1162.230	-967.944	1162.744	-955.373	1152.610
LTM Row 58	-129.890	107.954	-125.973	110.180	-127.025	109.513	-127.377	109.769	-130.990	107.068
LTM Row 59	-125.672	130.057	-121.905	125.346	-122.312	125.712	-122.174	125.777	-131.460	130.171
LTM Row 60	-10.191	13.442	-9.569	13.204	-9.566	13.240	-9.524	13.222	-9.852	13.088
LTM Row 61	-82.391	106.257	-78.834	104.746	-78.594	104.871	-78.735	104.794	-78.305	103.591
LTM Row 62	-24.076	121.615	-23.033	112.885	-23.030	112.838	-23.201	112.810	-23.362	113.540
LTM Row 63	-72.986	80.180	-74.006	79.146	-74.254	79.043	-74.308	79.096	-73.436	77.057
LTM Row 64	-2733.788	1981.400	-2768.411	1955.748	-2778.460	1962.435	-2779.020	1969.346	-2696.461	1998.610
LTM Row 65	-1986.944	2390.924	-1993.600	2403.396	-1989.133	2392.075	-1988.896	2393.278	-1955.770	2286.105
LTM Row 66	-997.770	1339.519	-892.090	1186.780	-890.659	1199.413	-894.419	1204.604	-809.017	1233.651
LTM Row 149	-20.023	21.690	-9.954	11.891	-9.766	11.829	-9.916	11.700	-13.832	14.085
LTM Row 150	-83.035	81.520	-61.647	52.603	-62.227	57.756	-61.261	59.241	-81.855	71.202
LTM Row 151	-16.768	13.490	-9.358	6.927	-9.768	7.056	-9.832	6.998	-12.200	10.020
LTM Row 152	-194.704	230.869	-160.975	157.300	-159.737	153.479	-159.591	148.885	-175.957	172.856
LTM Row 153	-91.644	131.848	-94.615	115.442	-96.752	115.962	-97.676	114.795	-114.314	137.597
LTM Row 154	-101.074	77.361	-63.852	61.391	-69.744	62.328	-71.259	61.854	-85.486	86.363
LTM Row 155	-37.265	49.875	-27.195	37.518	-26.767	37.609	-26.729	37.616	-36.476	45.999
LTM Row 156	-17.823	24.791	-16.363	19.037	-16.361	19.043	-16.262	18.948	-21.151	23.945

TABLE 3 STS-26 PAYLOAD/ORBITER INTERFACE LOADS (lbs)

1	2		3		4		5		6	
	Diagonal TMP		1 Iteration		2 Iterations		Full Damp-Matrix		1% System Damping	
ITEMS	Min	Max	Min	Max	Min	Max	Min	Max	Min	Max
X=1061.13 RHS Long 8000 X	-2999.701	1267.436	-3057.462	1352.655	-3082.049	1367.236	-3083.571	1367.911	-3792.084	2126.967
X=1061.13 RHS Long 8000 Z	-4003.971	7727.583	-4010.486	7748.758	-4009.231	7741.651	-4007.610	7745.237	-3924.981	7627.289
X=1155.53 RHS Long 43 X	-59543.562	-8938.251	-59761.283	-9024.557	-59758.595	-9024.424	-59763.502	-9028.895	-59733.092	-8909.008
X=1155.53 RHS Long 43 Z	-5003.924	563.117	-4994.387	569.692	-4994.234	565.773	-4991.766	566.079	-5010.085	576.838
X=1165.36 RHS Long 131 Y	-1830.120	4965.188	-2032.299	4792.680	-2021.604	4804.361	-2022.277	4803.494	-2360.679	5478.094
X=1216.50 RHS Long 132 Y	-3400.066	2104.577	-3184.771	2227.027	-3210.368	2223.260	-3206.910	2224.188	-3397.255	2215.780
X=1226.50 RHS Long 39 Z	-3742.837	587.852	-3738.841	592.606	-3736.534	589.249	-3736.319	589.928	-3726.953	582.139
X=1061.13 LHS Long 8250 X	-2900.900	1420.706	-2861.693	1444.388	-2864.546	1451.309	-2865.230	1451.446	-3891.571	1977.441
X=1061.13 LHS Long 8250 Z	-3491.037	8789.977	-3478.651	8811.324	-3484.214	8812.158	-3482.048	8811.452	-3505.514	8698.271
X=1155.53 LHS Long 124 X	-58111.550	-7810.329	-58197.228	-7630.843	-58199.854	-7624.490	-58198.757	-7622.496	-58203.158	-7822.706
X=1155.53 LHS Long 124 Z	-5216.399	964.893	-5198.748	956.545	-5198.593	954.800	-5196.326	955.384	-5204.973	950.756
X=1165.36 LHS Long 135 Y	-4103.196	1731.748	-4086.695	1573.935	-4083.623	1574.735	-4080.749	1575.901	-4679.327	1836.701
X=1216.50 LHS Long 136 Y	-2056.957	3773.966	-2001.451	3668.729	-2002.433	3676.866	-2002.596	3677.055	-2261.874	4056.924
X=1226.33 LHS Long 128 Z	-3799.106	918.146	-3802.587	913.438	-3803.697	911.633	-3802.116	911.518	-3800.477	905.737
X=1061.13 C/L Keel 8050 X	-2066.167	975.528	-2053.556	1056.768	-2053.922	1059.102	-2053.671	1059.239	-2295.171	1283.621
X=1061.13 C/L Keel 8050 Y	-2454.776	5073.594	-2460.642	4932.092	-2461.763	4947.572	-2461.972	4934.895	-2408.746	4939.606

TABLE 4 STS-26 IUS MOTOR ACCELERATIONS (g)

1	2		3		4		5		6	
	Diagonal TMP		1 Iteration		2 Iterations		Full Damp-Matrix		1% System Damping	
ITEMS	Min	Max	Min	Max	Min	Max	Min	Max	Min	Max
Small IUS Motor #3457 X	0.101	3.091	0.119	3.123	0.118	3.124	0.119	3.125	0.060	3.156
Small IUS Motor #3457 Y	-0.342	0.417	-0.188	0.228	-0.188	0.235	-0.181	0.238	-0.267	0.243
Small IUS Motor #3457 Z	-0.450	0.629	-0.470	0.610	-0.469	0.610	-0.470	0.611	-0.473	0.621
Small IUS Motor #3457 Rx	-1.916	1.726	-1.201	1.206	-1.192	1.267	-1.201	1.277	-1.735	1.590
Small IUS Motor #3457 Ry	-5.630	5.509	-5.889	4.998	-5.905	5.022	-5.903	5.012	-6.454	5.528
Small IUS Motor #3457 Rz	-1.849	1.439	-1.706	1.310	-1.753	1.420	-1.756	1.444	-2.410	1.950
Large IUS Motor #1331 X	0.423	2.735	0.416	2.754	0.416	2.754	0.416	2.754	0.418	2.727
Large IUS Motor #1331 Y	-0.183	0.319	-0.147	0.246	-0.149	0.244	-0.146	0.242	-0.195	0.281
Large IUS Motor #1331 Z	-0.510	0.506	-0.518	0.510	-0.518	0.510	-0.518	0.510	-0.514	0.500
Large IUS Motor #1331 Rx	-1.255	1.236	-1.269	1.433	-1.261	1.456	-1.258	1.458	-1.345	1.742
Large IUS Motor #1331 Ry	-2.246	2.395	-2.332	2.421	-2.321	2.416	-2.319	2.427	-2.596	2.714
Large IUS Motor #1331 Rz	-4.069	4.315	-2.261	2.384	-2.270	2.423	-2.179	2.313	-4.045	4.218

TABLE 5 STS-26 PAYLOAD/ORBITER INTERFACE ACCELERATIONS (g)

1	2		3		4		5		6	
	Diagonal TMP		1 Iteration		2 Iterations		Full Damp-Matrix		1% System Damping	
ITEMS	Min	Max	Min	Max	Min	Max	Min	Max	Min	Max
X=1061.13 RHS Long 8000 X	-2.537	-0.451	-2.533	-0.475	-2.532	-0.474	-2.532	-0.474	-2.762	-0.342
X=1061.13 RHS Long 8000 Z	-1.518	1.618	-1.510	1.591	-1.509	1.593	-1.510	1.592	-1.611	1.844
X=1155.53 RHS Long 43 X	-2.390	-0.303	-2.318	-0.299	-2.318	-0.299	-2.319	-0.299	-2.601	-0.199
X=1155.53 RHS Long 43 Z	-1.214	1.257	-1.216	1.187	-1.216	1.193	-1.215	1.190	-1.705	1.915
X=1165.36 RHS Long 131 Y	-2.735	2.437	-2.669	2.500	-2.672	2.498	-2.671	2.498	-2.807	2.651
X=1216.50 RHS Long 132 Y	-3.480	3.396	-3.461	3.359	-3.465	3.365	-3.464	3.364	-3.988	3.914
X=1226.33 RHS Long 39 Z	-1.267	1.401	-1.242	1.323	-1.234	1.328	-1.234	1.326	-2.061	2.227
X=1061.13 LHS Long 8250 X	-2.799	-0.346	-2.752	-0.367	-2.756	-0.366	-2.755	-0.366	-3.085	-0.217
X=1061.13 LHS Long 8250 Z	-1.466	1.534	-1.452	1.519	-1.453	1.521	-1.452	1.521	-1.555	1.771
X=1155.53 LHS Long 124 X	-2.535	-0.190	-2.524	-0.220	-2.526	-0.219	-2.526	-0.219	-2.776	-0.108
X=1155.53 LHS Long 124 Z	-1.097	1.275	-1.035	1.236	-1.043	1.237	-1.042	1.237	-1.788	1.962
X=1165.36 LHS Long 135 Y	-2.426	2.570	-2.328	2.509	-2.333	2.510	-2.333	2.510	-2.659	2.555
X=1216.50 LHS Long 136 Y	-3.045	3.427	-2.870	3.321	-2.888	3.326	-2.886	3.326	-3.457	3.790
X=1226.33 LHS Long 128 Z	-1.130	1.353	-1.043	1.272	-1.058	1.288	-1.057	1.286	-2.056	2.100
X=1061.13 C/L Keel 8050 X	-6.632	3.514	-6.497	3.577	-6.507	3.594	-6.507	3.595	-8.257	5.201
X=1061.13 C/L Keel 8050 Y	-0.292	0.338	-0.294	0.303	-0.292	0.301	-0.292	0.300	-0.326	0.436

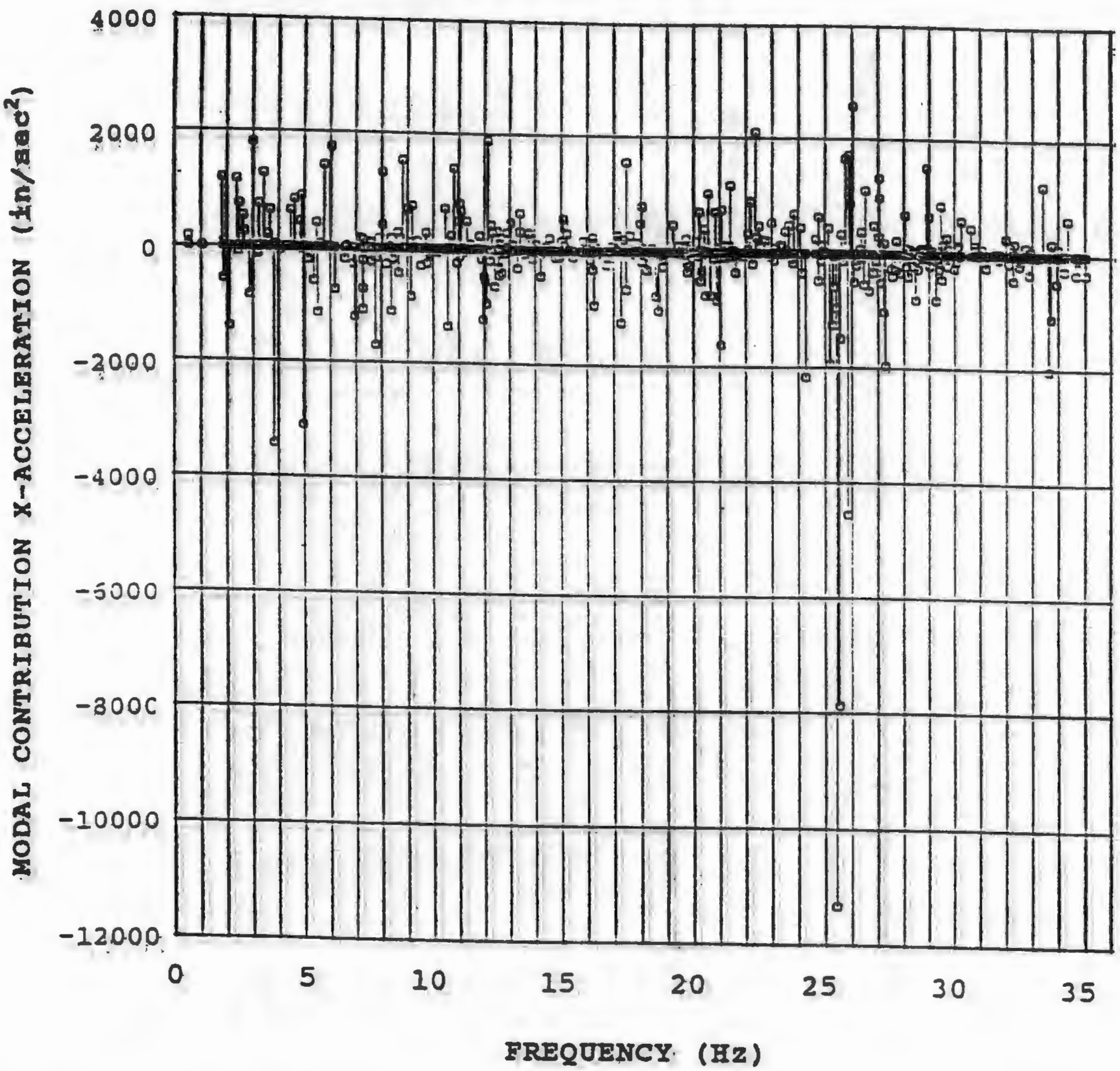

Figure 1 MODAL CONTRIBUTIONS FOR X-ACCELERATION (in/sec^2) OF STS-26 SA ANTENNA RIBS USING TMP METHOD, t=8.3 sec.

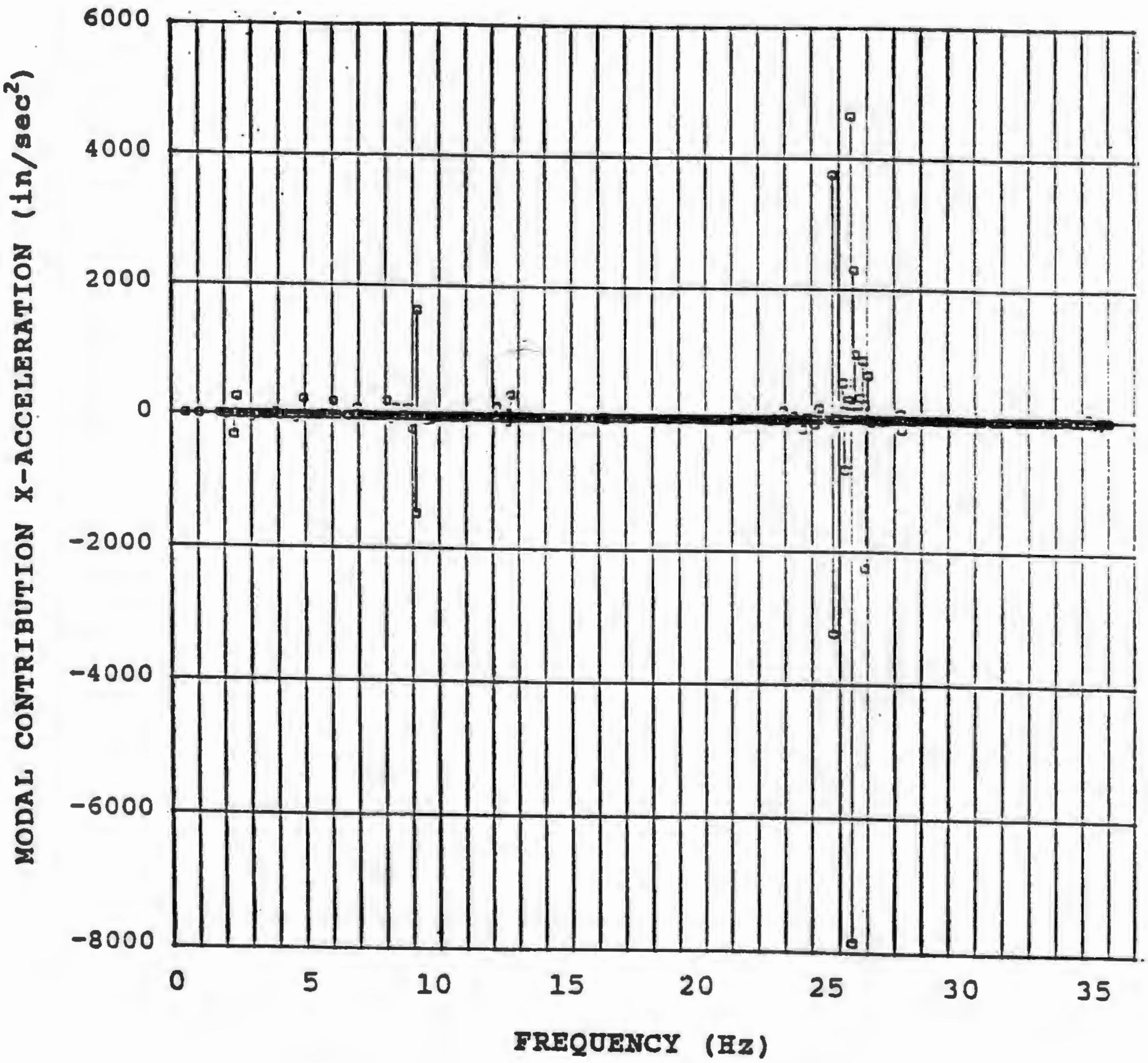

Figure 2 MODAL CONTRIBUTIONS FOR X-ACCELERATION (in/sec^2) OF STS-26 SA ANTENNA RIBS USING ITERATIVE METHOD t=8.3 sec.

U.S. Government Printing Office 548-076